Whitmarsh, R.B., Sawyer, D.S., Klaus, A., and Masson, D.G. (Eds.), 1996
Proceedings of the Ocean Drilling Program, Scientific Results, Vol. 149

19. CLAY MINERAL FABRICS FROM THE IBERIA ABYSSAL PLAIN: RECORDERS OF POSTRIFT CONSOLIDATION AND DEFORMATION?[1]

Julia K. Morgan[2]

ABSTRACT

Clay mineral fabrics in clay-rich sediments, collected from drill cores at Sites 897, 898, and 899 in the Iberia Abyssal Plain, were measured using the method of X-ray texture goniometry, to examine the relationships between fabric, strain, and physical properties, and to look for evidence for fabric changes induced by horizontal shortening of the abyssal sediments during Miocene compression. No evidence was found to support the idea that the sediments experienced horizontal ductile strain during their residence, although there was evidence for increasing fabric magnitude with depth, associated with burial and dewatering. A crude, approximately linear, relationship is inferred between discrete water contents and apparent volumetric strains derived from the measured fabric, which may correlate with fabric-strain relationships observed in other settings.

INTRODUCTION

Marine sediments can be sensitive indicators of events of global, regional, and local importance, by virtue of their chemical, lithologic, and physical properties. One underappreciated aspect of fine-grained sediments, particularly those containing significant concentrations of clay minerals, is their tendency to display textural characteristics that can be unique to their environment of deposition, diagenesis, or deformation (e.g., Moon and Hurst, 1984; Bennett et al., 1991). Several recent studies have taken special interest in the fabrics of clay-bearing sediments deposited (and deformed) in modern or ancient marine environments (e.g., Behrmann, 1991; Taylor et al., 1991; O'Brien et al., 1993; Paterson et al., 1995), particularly those that have become incorporated in accretionary prisms (Behrmann and Kopf, 1993; Morgan and Karig, 1993; Housen and van der Pluijm, 1994) as these sediments may preserve subtle deformation fabrics key to interpreting the kinematics of these moderately deformed domains.

The interest generated in the study of sediment fabrics arises from the presence of minerals with extreme aspect ratios (e.g., clay platelets or magnetite needles) that tend to rotate as the material compacts (e.g., Maltman, 1984; Moon and Hurst, 1984; Bennett et al., 1991). Sediments that are normally consolidated in a sedimentary basin will tend to display minerals that are preferentially oriented parallel or subparallel to the bedding plane, a configuration induced by uniaxial strain and dewatering during burial. Subsequent compression in the horizontal plane may produce continued ductile grain flow, causing these platy or elongate minerals to rotate toward an orientation perpendicular to the applied compressive stress (e.g., Oertel, 1983, 1985). If the resulting orientation distribution of grains can be quantified, and the relationship between the fabrics and the applied strain established, then this textural information can provide valuable information regarding sediment strain and regional deformation.

The Iberia Abyssal Plain provides an interesting setting in which to explore the nature of clay mineral fabrics and their kinematic relationships. The postrift setting of the Iberia Abyssal Plain adjacent to the Iberian passive margin led to the accumulation of a thick sequence of fine-grained sediments, deposited in a relatively quiescent environment (e.g., Sawyer, Whitmarsh, Klaus, et al., 1994). This provides an ideal combination for exploring the relationships between the development of fabric, the depth of burial, and the physical properties of the sediment. Moreover, the Iberia Abyssal Plain experienced a brief episode of postrift compression, associated with the Miocene Betic-Rif event, which resulted in broad folding of sediments in the Iberia Abyssal Plain, apparent on marine seismic reflection profiles (Mauffret et al., 1989; Masson et al., 1994). Rare compressional microfaults observed in drill cores from Leg 149 (e.g., Sawyer, Whitmarsh, Klaus, et al., 1994) may also have been introduced during this event. If the horizontal deformation associated with this compression produced sediment grain flow and mineral reorientation as has been interpreted in tectonically deformed accretionary prisms (Hounslow, 1990; Morgan and Karig, 1993; Owens, 1993; Housen and van der Pluijm, 1994), then a record of this event may be preserved in the sediment fabric.

The objective of this study is to explore the relationship between sediment fabric, physical properties, and deformational history using several tools. Quantifying clay mineral fabrics is a major emphasis, and for this purpose, the technique of X-ray texture goniometry (XTG) is used (Cullity, 1978; Wenk, 1985). These fabrics are correlated to discrete laboratory index property measurements obtained from the same samples. This information can help to delineate the bulk finite strain the sediment experienced in the Iberia Abyssal Plain, and possibly establish regional variations in fabric and other physical properties across the abyssal plain. In addition, this study adds to an accumulating database of clay mineral fabrics quantified using XTG, derived from both tectonic and nontectonic settings (e.g., Paterson et al., 1995), and will assist in efforts to better understand the mechanisms involved in fabric development in various environments.

METHOD OF STUDY

Sample Selection

Sediment cores obtained from the Iberia Abyssal Plain during Leg 149 displayed multiple lithologies, which undoubtedly represented a wide range of fabrics and physical properties (e.g., Sawyer, Whitmarsh, Klaus, et al., 1994). For the purposes of this study, it was important to obtain samples which were compositionally and texturally similar, and ones that were relatively clay-rich (e.g., more than 30% clay minerals), so as to minimize the factors that might influence the

[1]Whitmarsh, R.B., Sawyer, D.S., Klaus, A., and Masson, D.G. (Eds.), 1996. *Proc. ODP, Sci. Results,* 149: College Station, TX (Ocean Drilling Program).
[2]Department of Geological Sciences, University of Washington, Seattle, WA 98195, U.S.A. morgan@geology.washington.edu.

development of mineral fabrics. Throughout much of the section, thin interbedded silty claystones and clayey siltstones occurred in beds from several centimeters to meters thick. The samples chosen for this study were selected from such layers which displayed at least 5 cm of relatively uniform, homogeneous, cohesive material. This provided material enough to prepare two mutually perpendicular X-ray sections, to perform a series of index property measurement, and, it is hoped, to eventually obtain corresponding paleomagnetic and magnetic fabric measurements. Several samples were selected to coincide with samples taken for shipboard index property measurements to allow for direct comparison of laboratory and shipboard analyses.

Because of the need for cohesive samples, only sediments below about 200 m below seafloor (mbsf) were selected from any given hole. Most of the samples were collected from depths ranging between about 250 and 350 mbsf; deeper samples were obtained only from Hole 897B. In hindsight, given the coherent nature of these muds, more samples could have been taken from the shallower cores, thereby permitting better extrapolation of fabric trends into these shallow levels. Samples were taken at Sites 897, 898, and 899; Site 900 was not sampled because of the high degree of lithification (cementation), which may have influenced the sediment porosity (Shipboard Scientific Party, 1994b), and possibly limited the clay mineral rotations which yield the preferred orientations. Perhaps future studies will be targeted toward exploring these relationships.

All told, 20 quarter-round samples were taken for this study, over depths ranging between 180 and almost 600 mbsf; 18 of these samples were analyzed. Most samples were typical of grayish green or olive-green silty clay layers, collected from Lithostratigraphic Units IIA and IIB (Sawyer, Whitmarsh, Klaus, et al., 1994). Several samples tended more towards reddish brown claystones near the base of Unit IIB.

X-ray Sample Preparation and Analysis

Methods for X-ray sample preparation, analysis, and data reduction generally follow those described previously in an earlier paper describing clay-mineral fabric analyses from the Nankai Trough and prism (Morgan and Karig, 1993); the complete details of these methods will not be repeated here. However, briefly, two mutually perpendicular sections, each containing the vertical axis of the core were trimmed for each sample, and impregnated with epoxy resin (LR White) prior to sectioning and mounting for X-ray work. Sections 200-300 μm thick were prepared on aluminum chips with a 1-cm-diameter hole for X-ray scans in transmission mode.

X-ray scans were conducted on a Scintag SPF-105, located in the Materials Science Center at Cornell University, using a molybdenum X-ray source. This source was chosen over the previously used copper source because of its higher signal-background ratios (van der Pluijm et al., 1994). Scans were conducted on a combined reflection for chlorite (002) and kaolinite (001). This combined peak consistently provided the most distinct phyllosilicate reflection in these samples. Peak intensities were corrected for background, assumed to be 95% of the X-ray intensities measured at about 6.5° 2θ; X-ray intensities measured in this position showed very little dependence on the density of the clay phase (Morgan and Karig, 1993). In addition, the intensity of the clay reflections was corrected for variations in volume of the irradiated sample and sample tilt using variations in this inferred background taken about 2° 2θ above the peak reflection (e.g., Bragg and Packer, 1963; 1964). The resulting intensities, corrected for background and tilt, will be proportional to the density of clay minerals favorably oriented to diffract X-rays in that position (Oertel, 1983; Wenk, 1985).

The background and tilt corrections introduce the greatest uncertainties in the determination of the mineral fabric, because of poor constraints on the factors that affect X-ray absorption and background signal in fine-grained, multiphase sediments. X-ray absorption depends principally on the composition of the material and length of the beam path, and slight heterogeneities in microstructure and sample thickness might introduce very slight effects. Background determination is most problematic in these sediments, as stacking disorders and finite grain size may cause significant broadening of clay reflections; true background may never be observed in the diffraction pattern (Brindley, 1980). Moreover, low clay contents and mixed composition result in low signal to noise ratios, increasing the uncertainty in the magnitude of the corrected intensity. A detailed discussion and justification of the corrections used here are given in Morgan and Karig (1993).

X-ray scans took, on average, 8 hr to perform, counting X-ray intensities at both peak and background positions for approximately 75 s each. Each X-ray section was rotated and tilted within the beam to measure peak and background intensities over a range of orientations, yielding two intersecting cones of data subtending 70°, centered about the plane of the section. When plotted on a lower-hemisphere equal-area projection, this yields two perpendicular bands of data that overlap to provide nearly complete, spherical density distribution for the sample (e.g., Morgan and Karig, 1993).

The two perpendicular, background- and tilt-corrected intensity distributions are combined, and a best-fit density distribution calculated, assuming an orthorhombic form consistent with the passive rotation of randomly oriented planar elements in the sediment, (e.g., March model; March, 1932; Oertel, 1985). The principal densities calculated this way can be inverted to principal March strains, ε_i, and stretches, S_i, as follows:

$$S_i = (1 + \varepsilon_i) = \rho_i^{-1/3} \quad (i = 1, 2, 3), \tag{1}$$

where ρ_i are the principal densities of clay minerals determined from the fitting routine. The goodness of fit of the resulting density distribution can be qualitatively evaluated by comparing the combined distribution with those determined for the individual scans (Fig. 1), and the fit depends on the use of appropriate corrections to the raw intensity data (see above; Morgan and Karig, 1993). In order to express the uncertainties in the determination of the March stretches, fabric parameters calculated from these quantities are presented for both the individual and combined scans, with the former defining the range of possible values, and the latter representing the best estimate for the sediment.

Arguments for the appropriateness of the March model for fabric development have been taken up elsewhere (Holeywell and Tullis, 1975; Siddans, 1976; Etheridge and Oertel, 1979), and will not be considered here. However, March strains and stretches do present useful quantities for describing mineral fabrics in the context of strains that may have been responsible for them, and they will be used in this context here. Moreover, one of the long-term objectives of this type of study is to test these fabric-strain relationships.

Index Property Measurements

In addition to the fabric measurements described above, portions of samples taken for this study were put aside for index property measurements, specifically for determining water content, grain density, and porosity. Raw measurements made include wet mass, dry mass, and dry volume. Wet volume was not measured, precluding independent measures for bulk density in this suite of measurements. However, the available quantities permit not only direct correspondence with fabric estimations, but also opportunity to test shipboard measurements.

Wet and dry mass were measured using a balance, before and after drying samples in a 120°C oven for 48 hr. Dry volume of the powdered sample was measured using a flask pycnometer maintained at a constant temperature of 60°C in a water bath. Pycnometer measure-

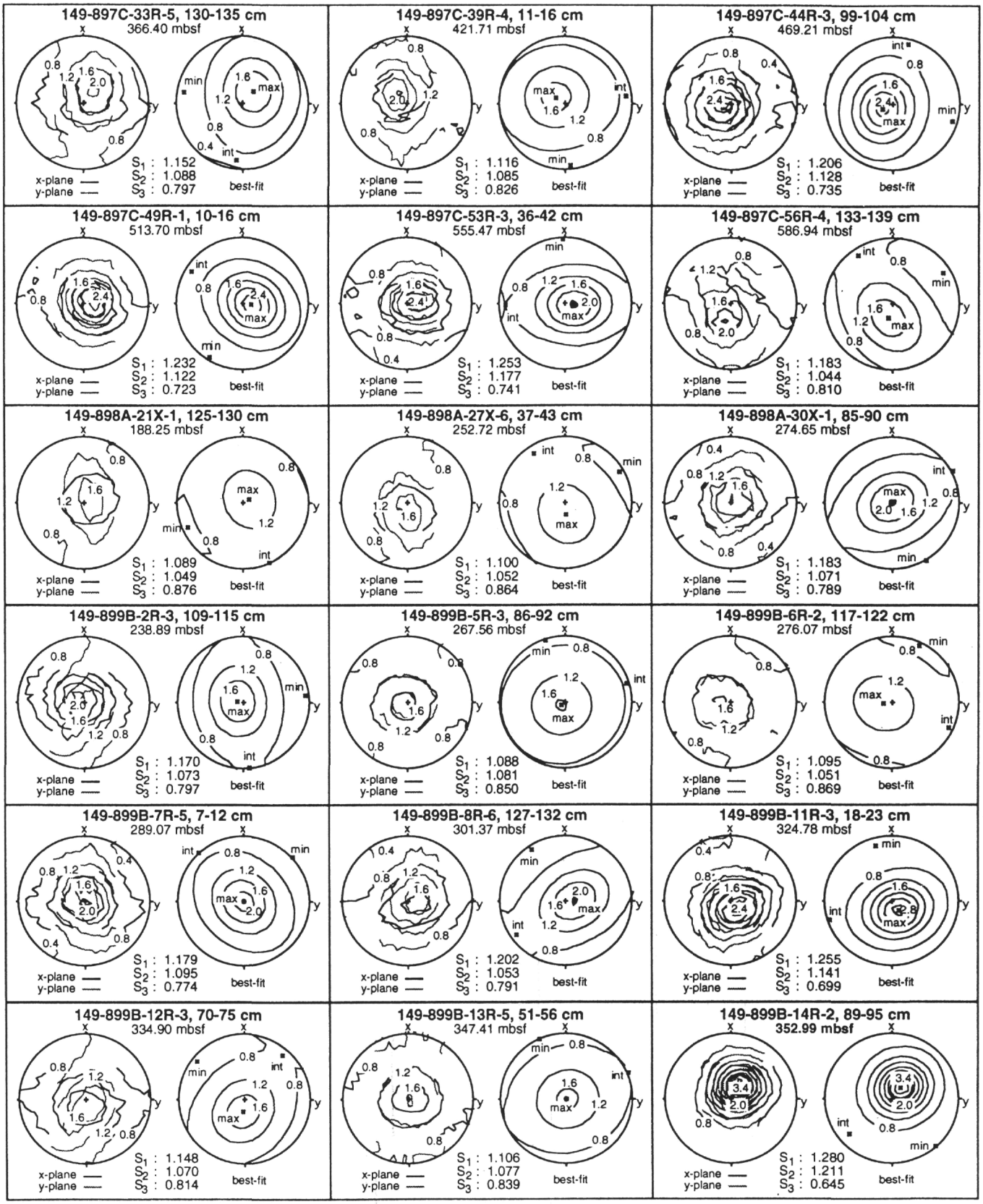

Figure 1. Pole figures for the 18 samples collected using XTG methods. In each box, the left figure shows the raw data for the *x*- and y-planes, displayed as solid and shaded lines respectively, and demonstrates goodness of fit or mismatch. The right figure represents the best-fit composite pole figure calculated for the combined *x*- andy-scans. Contours of clay mineral density are given in multiples of random distribution. The tabulated values in each box represent the normalized principal March stretches for the combined pole figure.

ments were made with less than ideal equipment, so it proved difficult to control the flask volume accurately. This uncertainty introduces significant error into the estimates for volume of small quantities of powder, possibly up to 15% error in dry volume measurements, evidenced by the calculated density values.

The raw measurements permit calculation of several useful quantities, including water content, grain density, and porosity. Water content is defined as

$$W_c = M_w/M_t \ , \tag{2}$$

where $M_w = M_t - M_d$ is the mass of the water, and M_t and M_d are the sample wet and dry mass, respectively. Grain density is derived as

$$\rho_g = M_g/V_g \ , \tag{3}$$

where M_g and V_g are the grain mass and volume, respectively. These quantities, calculated from the dry mass and volume V_d must be corrected for salt content of the evaporated water as $M_g = M_d - 0.035M_w$, and $V_g = V_d - 0.035M_w/\rho_s$ where ρ_s is the density of salt, and assumed to be 2.257 g/cm^3.

Porosities can be derived from these quantities as follows:

$$\eta = \frac{M_w}{M_w - (\rho_w/\rho_g)M_g} , \tag{4}$$

Several alternative calculations are possible for porosity, depending on the raw data available (Shipboard Scientific Party, 1994a), and the results are not always identical. This lack of internal consistency in Ocean Drilling Program shipboard index properties was noted previously (Morgan and Karig, 1995); porosities calculated using bulk density and grain density, as were the Leg 149 shipboard data (Sawyer, Whitmarsh, Klaus, et al., 1994), are consistently slightly lower than those calculated using the above relationship.

RESULTS

Clay Mineral Fabrics

The resulting measured and best-fit pole figures obtained for the suite of samples analyzed here, and the calculated March stretches, are displayed in Figure 1, showing the variation in shape and intensity between perpendicular sections, and among the samples. These figures are difficult to evaluate individually, but the fabric defined by the March stretches can be described by several derived parameters, such as lateral and total anisotropy, strain ellipsoid shape factor, and apparent volumetric strain.

Lateral anisotropy, defined as

$$A_3 = \frac{S_1 - S_2}{S_1 + S_2} \cdot 200\% , \tag{5}$$

describes the degree of fabric eccentricity in the horizontal plane (e.g., the deviation of the mineral preferred orientation in the horizontal plane from a circularly symmetric distribution). Total anisotropy,

$$A_3 = \frac{S_1 - S_3}{S_1 + S_2 + S_3} \cdot 300\% , \tag{6}$$

describes the difference in maximum and minimum stretches, normalized to the mean stretch; in the case of nearly uniaxial strain in a sedimentary basin, it describes the degree of flattening of the fabric ellipsoid.

Lateral and total anisotropy are plotted against depth in Figure 2. Lateral anisotropy plots generally between 0% and 15%, with a certain amount of scatter. There is little systematic variation with depth, either within a given hole or for the entire suite, at least where the data density is greatest (250-350 mbsf). The deeper samples, all derived from Site 897, suggest some slight increase with depth, perhaps up to 12%-15%, but the points are too few and the error too great in this range to permit a meaningful interpretation. From the appearance of this noisy data set, lateral anisotropy varies little with depth, with an average value of 6.53% for the data points representing the combined scans. This average is less than the lateral anisotropy of 10% reported for moderately deformed sediments from the toe of the Nankai accretionary prism (Morgan and Karig, 1993), and probably lies within the error of the X-ray measurements. It does not provide compelling evidence for lateral strain in this setting.

Total anisotropy also shows significant scatter in the depth plot (Fig. 2), ranging between about 20% and 60%. The highest values, for Samples 149-899B-11R-3, 18-23 cm, at 325 mbsf, and 149-899B-14R-2, 89-95 cm, at about 353 mbsf, are isolated from the rest of the data, and appear to be anomalous. The remaining samples show a slight tendency for total anisotropy to increase with depth. Such an increase in total anisotropy with depth is consistent with increased flattening of the sediment and the progressive rotation of clay minerals toward the horizontal plane during burial (e.g., Moon and Hurst, 1984).

A parameter used to describe the shape of the fabric (or strain) ellipsoid is the fabric ellipsoid shape factor, derived from the classic Flinn diagram, and defined as

$$k = \frac{S_1/S_2 - 1}{S_2/S_3 - 1} . \tag{7}$$

This shape factor varies from a value of zero for a perfectly oblate (flattened) ellipsoid, to infinity for a perfectly prolate (constricted) one. For our suite of samples, k lies generally within the oblate field (Fig. 3), $0 < k < 1$, ranging between 0.0 and 0.6, and demonstrates a strain history dominated by the uniaxial flattening incurred during basinal consolidation.

X-ray goniometry and the derived March strains document the relative magnitudes of mineral densities or strains, and therefore are independent of volume strain. However, if the history of sediment deformation is one dominated by uniaxial strain as suggested by the lateral anisotropy and shape factor, then the lateral stretches should be unity (e.g., no strain). It is then possible to calculate an apparent volume strain. The principal stretches are normalized by the geometric average of the lateral stretches, and volume strain, is determined from the product of the normalized stretches:

$$\Delta_F = 1 - \frac{S_1 S_2 S_3}{\sqrt{S_1 S_2}} , \tag{8}$$

(contractional strain is assumed to be positive). The resulting plot (Fig. 4) suggests that the volumetric strain of sediments actually increases downward, as would be expected for sediments dewatering during uniaxial consolidation and burial. Two stand out from the rest of the data points with anomalously high apparent volume strains, denoting well developed mineral fabrics. The apparent volumetric strain ranges from about 0.17 for the shallowest samples to about 0.35-0.40 for the deeper ones.

Index Properties

Water content, grain density, and porosity were calculated for the samples examined above and the results are listed in Table 1. Several shipboard index property samples were taken adjacent to the

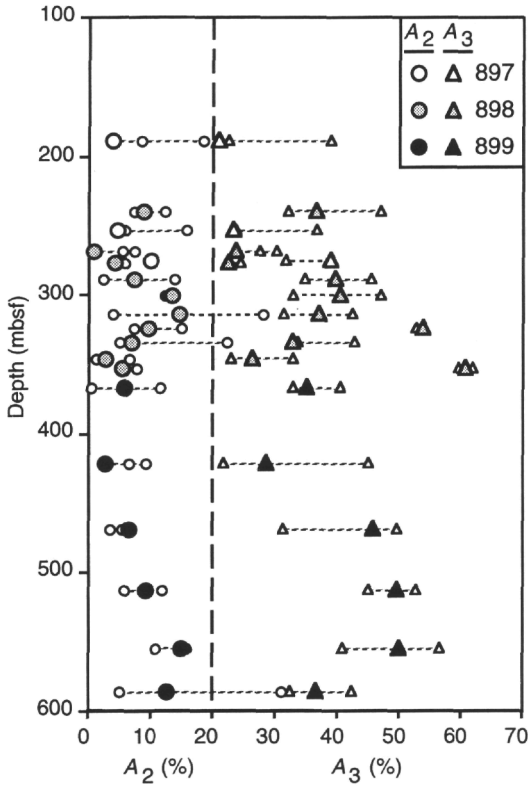

Figure 2. Lateral anisotropy (A_2-circles) and total anisotropy (A_3-triangles) calculated from the March stretches, plotted vs. depth for all samples. Three data points are given for each sample: the large symbols represent the best-fit "average," calculated from the combination of the individual x and y data sets; the small symbols connected by dashed lines denote the values obtained for each scan, and provide an estimate of the error in these measurements. Because of the weighting of individual data points, the best-fit value may not correspond to the mean; if the scans yield fabrics with conflicting orientations, the best-fit value may lie outside the range defined by the independent scans.

fabric samples, permitting the results to be compared directly. The derived quantities are also plotted with the shipboard measurements in Figure 5.

Laboratory water contents correspond quite well to those obtained shipboard, with the exception of several points. This demonstrates that the samples did not dry out significantly during storage. Grain densities do not fit nearly as well, and laboratory values show significant scatter. As mentioned above, this error arises from relatively crude pycnometer measurements, and does not reflect the true variability in grain densities. Porosities were calculated using both the measured grain densities (open symbols), and inferred grain density of 2.8 g/cm^3 estimated from the shipboard measurements (solid symbols). The latter values tend to lie just above the cloud of data obtained during the cruise (the offset is attributed to the different methods used to calculate the porosities, discussed above) with deviations tied closely to the variations in water content. In summary, the index properties, with the exception of laboratory grain densities give reasonable estimates for the discrete properties of the fabric samples.

Correlation between Fabric and Index Properties

Water content in the sediment is in part a function of volumetric sediment strain, so as sediments are buried their water contents drop. This volumetric change, Δ_w can be expressed in terms of W_c and several other parameters,

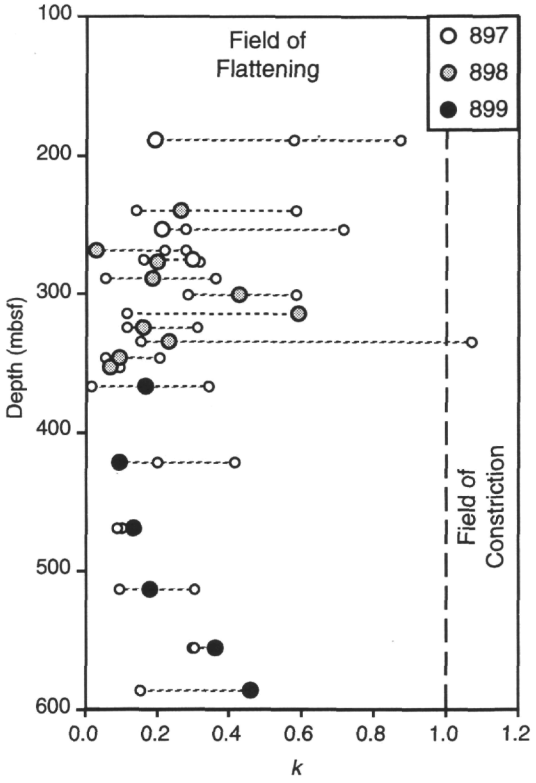

Figure 3. Fabric (strain) ellipsoid shape factor *(k),* calculated from the March stretches, plotted vs. depth for all samples. See Figure 2 caption for explanation of symbols.

$$\Delta_W = 1 - (V/V^0) = 1 - \frac{(\rho_w/\rho_g)V_g(W_c + 1)}{V_w^0 + V_g}, \qquad (9)$$

where V refers to the total sediment volume, and V^0 and V^0_w represent the reference (undeformed) sediment and water volumes, respectively. If we assume that the other parameters are approximately constant, a good first-order approximation for similar materials, then this complicated expression defines a linear relationship between volume strain and water content. Thus, a comparison of the apparent volume strain, Δ_F defined in equation (8) and measured water content will provide a meaningful way to evaluate the relationship between fabric and strain.

The two quantities are plotted against each other in Figure 6, and again, the plot shows significant scatter. However, there is a slight correlation between decreasing water content and increasing Δ_F, particularly within a given hole. Unfortunately, the range of measurements is narrow and the sampling size is small, preventing meaningful extrapolation of this linear relationship to either higher or lower water contents. Yet, these findings do suggest that a measurable relationship may exist between fabric and strain, which may be pinned down by more careful classification of sediments (e.g., with respect to lithology, clay concentration, and initial fabric), and by better constraining the uncertainties in the X-ray technique.

DISCUSSION

The fabric parameters plotted in Figures 2-4 all support a picture of sediments that have been uniaxially consolidated in a quiescent passive margin setting, undisturbed by any postdepositional bulk deformation. Even variations that might be attributed to differences in

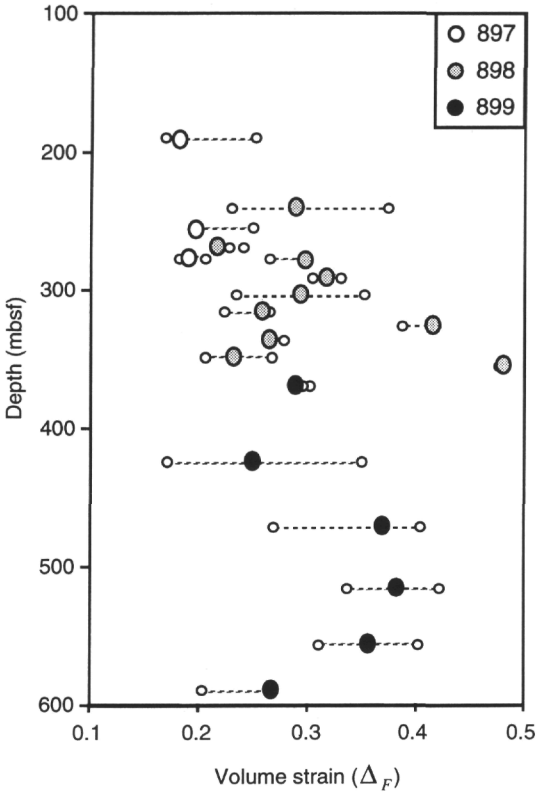

Figure 4. Apparent volume strain (Δ_F), calculated from March stretches normalized to zero lateral strain, plotted vs. depth. See Figure 2 caption for explanation of symbols.

initial fabric are not glaring. The absence of any significant lateral anisotropy attributed to the preferred orientation of clay minerals in the horizontal plane contrasts with the fabric of sediments from the toes of accretionary prisms (e.g., Morgan and Karig, 1993), where lateral anisotropy of about 10% indicates a component of lateral bulk shortening in these sediments.

This contrast probably reflects a distinct difference in mechanical state, in terms of stress magnitude and preferred modes of deformation. In accretionary prisms, horizontal tectonic stresses are inferred to be relatively high (Karig and Morgan, 1994) and appear to induce both ductile deformation by intergranular flow leading to mineral preferred orientation, and brittle deformation leading to abundant microfaults and throughgoing thrust faults. In the Iberia Abyssal Plain setting, far-field stresses do not appear to have caused significant grain flow, as evidenced by the poorly developed mineral fabrics; these compressional stresses are resolved instead through the formation of discrete microfaults identified in the drill cores, and broad folding observed on the reflection profiles.

The clay mineral fabrics detailed by this study, however, do show some sensitivity to compaction and dewatering during uniaxial consolidation and burial. There is a tendency for clay minerals to rotate toward parallelism with the bedding plane with depth, and a subtle, approximately linear relationship is suggested between water content and apparent strain derived from the fabric. There are still major uncertainties in primary sediment parameters, such as the initial fabric at the depositional surface, the initial water content, the concentration of clay minerals, as well as on the mechanisms of mineral rotation during strain. Some controls on these quantities may be gained through more complete examination of the sediments under consideration, and by experimental work where initial fabric, water content, and composition are precisely known and applied strains can be measured. However, such data has not been generated for this study. There are also uncertainties in the application of the X-ray technique, specifically with respect to determining true background and correction factors. Some progress is being made in this direction (e.g., van der Pluijm et al., 1994) and future efforts using modified equipment may elucidate some of these problems.

CONCLUSION

Clay mineral fabrics, measured in clay-rich sediments obtained from drill cores taken in the Iberia Abyssal Plain, show little evidence for lateral strain that may have been induced during regional compression in the Miocene. Expressions of this compressional event may be restricted to broad warping of sediments observed on seismic profiles, and to the occurrence of discrete microfaults with reverse displacement that were observed in drill cores.

Sediments do display a crude increase in fabric flattening with depth, consistent with the rotation of clay platelets toward the bedding plane during burial and compaction in a quiescent setting. Comparison of discrete index property measurements with apparent volume strains calculated from March strains suggest that there might be a linear relationship between fabric and water content. This relationship needs to be tested in sediments from other sites in order to clarify its character.

The results of this study contribute to continuing efforts to quantify the relationships between sediment fabric and strain, and add to the growing body of information on this subject, all dedicated toward extending our understanding of deformation mechanisms at work in the porous sediments which mantle the earth.

ACKNOWLEDGMENTS

The author wishes to thank Gerhard Oertel and Bernard Housen for thoughtful reviews, and Maura Weathers for assistance with the X-ray goniometer. This work was supported by grant USSSP022.

REFERENCES

Behrmann, J.H., 1991. Texturentwicklung in feinkörnigen, marinen Tongesteinen. Probenarbeitung ODP Legs 128 and 131 (Japan-See, Nankai). *Work. Rep., DFG Proj. Bel041/5-l "Tontexturen."*

Behrmann, J.H., and Kopf, A., 1993. Textures and microfabrics in fine-grained muds and mudstones from Site 808, Nankai accretionary prism. *In* Hill, I.A., Taira, A., Firth, J.V., et al., *Proc. ODP, Sci. Results,* 131: College Station, TX (Ocean Drilling Program), 45-56.

Bennett, R.H., O'Brien, N.R., and Hulbert, M.H., 1991. Determinants of clay and shale microfabric signatures: processes and mechanisms. *In* Bennett, R.H., Bryant, W.R., and Hulbert, M.H. (Eds.), *Microstructure of Fine-Grained Sediments: From Mud to Shale:* New York (Springer-Verlag), 5-32.

Bragg, R.H., and Packer, C.M., 1963. Effect of absorption and incoherent scattering on X-ray line profiles. *Rev. Sci. Instrumen.,* 34:1202-1207.

———, 1964. Quantitative determination of preferred orientation. *J. Appl Phys.,* 35:1322-1328.

Brindley, G.W., 1980. Order-disorder in clay mineral structures. *In* Brindley, G.W., and Brown, G. (Eds.), *Crystal Structures of Clay Minerals and Their X-ray Identification.* Mineral. Soc. Monogr. London, 5:125-195.

Cullity, B.D., 1978. *Elements of X-ray Diffraction:* Reading, PA (Addison-Wesley).

Etheridge, M.A., and Oertel, G., 1979. Strain measurements from Phyllosilicates—a precautionary note. *Tectonophysics,* 60:107-120.

Holeywell, R.C., and Tullis, T.E., 1975. Mineral reorientation and slaty cleavage in the Martinsburg Formation, Lehigh Gap, Pennsylvania. *Geol. Soc. Am. Bull.,* 86:1296-1304.

Hounslow, M.W., 1990. Grain fabric measured using magnetic susceptibility anisotropy in deformed sediments of the Barbados Accretionary Prism: Leg 110. *In* Moore, J.C., Mascle, A., et al., *Proc. ODP, Sci. Results,* 110: College Station, TX (Ocean Drilling Program), 257-275.

Housen, B.A., and van der Pluijm, B.A., 1994. Quantification of deformation fabrics in the Cascadia accretionary prism using magnetic anisotropy and X-ray texture goniometry. *Geol. Soc. Am. Abstr. Prog.,* 26:167.

Karig, D.E., and Morgan, J.K., 1994. Tectonic deformation: stress paths and strain histories. *In* Maltman, A. (Ed.), *The Geological Deformation of Sediments:* London (Chapman and Hall), 167-204.

Maltman, A., 1984. On the term "soft-sediment deformation." *J. Struct. Geol.,* 6:589-592.

March, A., 1932. Mathematische Theorie der Regelungen nach der Korngestalt bei affiner Deformation. *Z. Kristallogr., Mineral. Petrogr., Abt. A,* 1:285-297.

Masson, D.G., Cartwright, J.A., Pinheiro, L.M., Whitmarsh, R.B., Beslier, M.-O., and Roeser, H., 1994. Localized deformation at the ocean-continent transition in the NE Atlantic. *J. Geol. Soc. London,* 151:607-613.

Mauffret, A., Mougenot, D., Miles, P.R., and Malod, J.A., 1989. Cenozoic deformation and Mesozoic abandoned spreading centre in the Tagus abyssal plain (west of Portugal): results of a multichannel seismic survey. *Can. J. Earth Sci.,* 26:1101-1123.

Moon, C.F., and Hurst, C.W., 1984. Fabrics of muds and shales: an overview. *In* Stow, D.A.V., and Piper, D.J.W. (Eds.), *Fine-Grained Sediments: Deep-Water Processes and Facies.* Geol. Soc. Spec. Publ. London, 15:579-593.

Morgan, J.K., and Karig, D.E., 1993. Ductile strains in clay-rich sediments from Hole 808C: preliminary results using X-ray pole figure goniometry. *In* Hill, I.A., Taira, A., Firth, J.V., et al., *Proc. ODP, Sci. Results,* 131: College Station, TX (Ocean Drilling Program), 141-155.

———, 1995. Kinematics and a balanced and restored cross-section across the toe of the eastern Nankai accretionary prism. *J. Struct. Geol.,* 17:31-45.

O'Brien, D.K., Manghnani, M.H., Tribble, J.S., and Wenk, H.-R., 1993. Preferred orientation and velocity anisotropy in marine clay-bearing calcareous sediments. *In* Rezac, R., and Lavoie, D.L. (Eds.), *Carbonate Microfabrics:* New York (Springer), 149-161.

Oertel, G., 1983. The relationship of strain and preferred orientation of phyllosilicate grains in rocks—a review. *Tectonophysics,* 100:413-447.

———, 1985. Reorientation due to grain shape. *In* Wenk, H.-R. (Ed.), *Preferred Orientation in Deformed Metals and Rocks: An Introduction to Texture Analysis:* London (Acad. Press), 259-266.

Owens, W.H., 1993. Magnetic fabric studies of samples from Hole 808C, Nankai Trough. *In* Hill, I.A., Taira, A., Firth, J.V., et al., *Proc. ODP, Sci. Results,* 131: College Station, TX (Ocean Drilling Program), 301-310.

Paterson, S.R., Yu., H., and Oertel, G., 1995. Primary and tectonic fabric intensities in mudrocks. *Tectonophysics.* 247:105-119.

Sawyer, D.S., Whitmarsh, R.B., Klaus, A., et al., 1994. *Proc. ODP, Init. Repts.,* 149: College Station, TX (Ocean Drilling Program).

Siddans, A.W.B., 1976. Deformed rocks and their textures. *Philos. Trans. R. Soc. London A,* 283:43-54.

Shipboard Scientific Party, 1994a. Explanatory notes. *In* Sawyer, D.S., Whitmarsh, R.B., Klaus, A., et al., *Proc. ODP, Init. Repts.,* 149: College Station, TX (Ocean Drilling Program), 11-34.

———, 1994b. Site 900. *In* Sawyer, D.S., Whitmarsh, R.B., Klaus, A., et al., *Proc. ODP, Init. Repts.,* 149: College Station, TX (Ocean Drilling Program), 211-262.

Taylor, E., Burkett, P.J., Wackier, J.D., and Leonard, J.N., 1991. Physical properties and microstructural response of sediments to accretion-subduction: Barbados forearc. *In* Bennett, R.H., Bryant, W.R., and Hulbert, M.H. (Eds.), *Microstructure of Fine-Grained Sediments: From Mud to Shale:* New York (Springer), 213-228.

van der Pluijm, B.A., Ho, N.-C., Peacor, D.R., 1994. High-resolution X-ray texture goniometry. *J. Struct. Geol.,* 16:1029-1032.

Wenk, R.-H., 1985. Measurement of pole figures. *In* Wenk, H.-R. (Ed.), *Preferred Orientation in Deformed Metals and Rocks: An Introduction to Texture Analysis:* London (Academic), 11-72.

Date of initial receipt: 5 December 1994
Date of acceptance: 27 **March 1995**
149SR-233

Table 1. Selected index properties measured on discrete samples used for the fabric study.

Core, section, interval (cm)	Depth (mbsf)	Water content (%)	Grain density (g/m^3)	Porosity (%) (water content)	Porosity (%) (grain density)
149-897C-					
33R-5, 130–135 cm	366.40	35.36	2.96	50.80	49.46
39R-4, 11–16 cm	421.71	34.02	2.88	49.18	48.48
44R-3, 99–104 cm	469.29	31.98	N.A.	N.A.	46.92
49R-1, 10–16 cm	513.70	30.05	2.92	46.41	45.36
53R-3, 36–42 cm	555.47	34.68	2.83	49.24	48.97
56R-4, 133–139 cm	586.94	25.79	2.82	41.71	41.57
149-898A-					
21X-1, 125–130 cm	188.25	50.56	3.23	61.87	58.45
27X-6, 37–43 cm	252.72	40.46	2.88	53.58	52.87
30X-1, 85–90 cm	274.65	37.86	3.43	56.21	51.19
149-899B-					
2R-3, 109–115 cm	238.89	28.14	2.81	43.78	43.72
5R-3, 86–92 cm	267.56	34.28	2.91	49.63	48.67
6R-2, 117–122 cm	276.07	36.94	3.00	52.29	50.56
7R-5, 7–12 cm	289.07	39.93	3.31	56.67	52.53
8R-6, 127–132 cm	301.37	35.70	2.96	51.08	49.70
10R-2, 135–141 cm	314.85	31.72	2.80	46.67	46.72
11R-3, 18–23 cm	324.78	32.29	2.54	44.69	47.16
12R-3, 70–75 cm	334.90	29.42	2.94	46.00	44.82
13R-5, 51–56 cm	347.41	27.04	2.77	42.45	42.73
14R-2, 89–95 cm	352.99	28.52	2.80	44.01	44.05

Note: N.A. = not available.

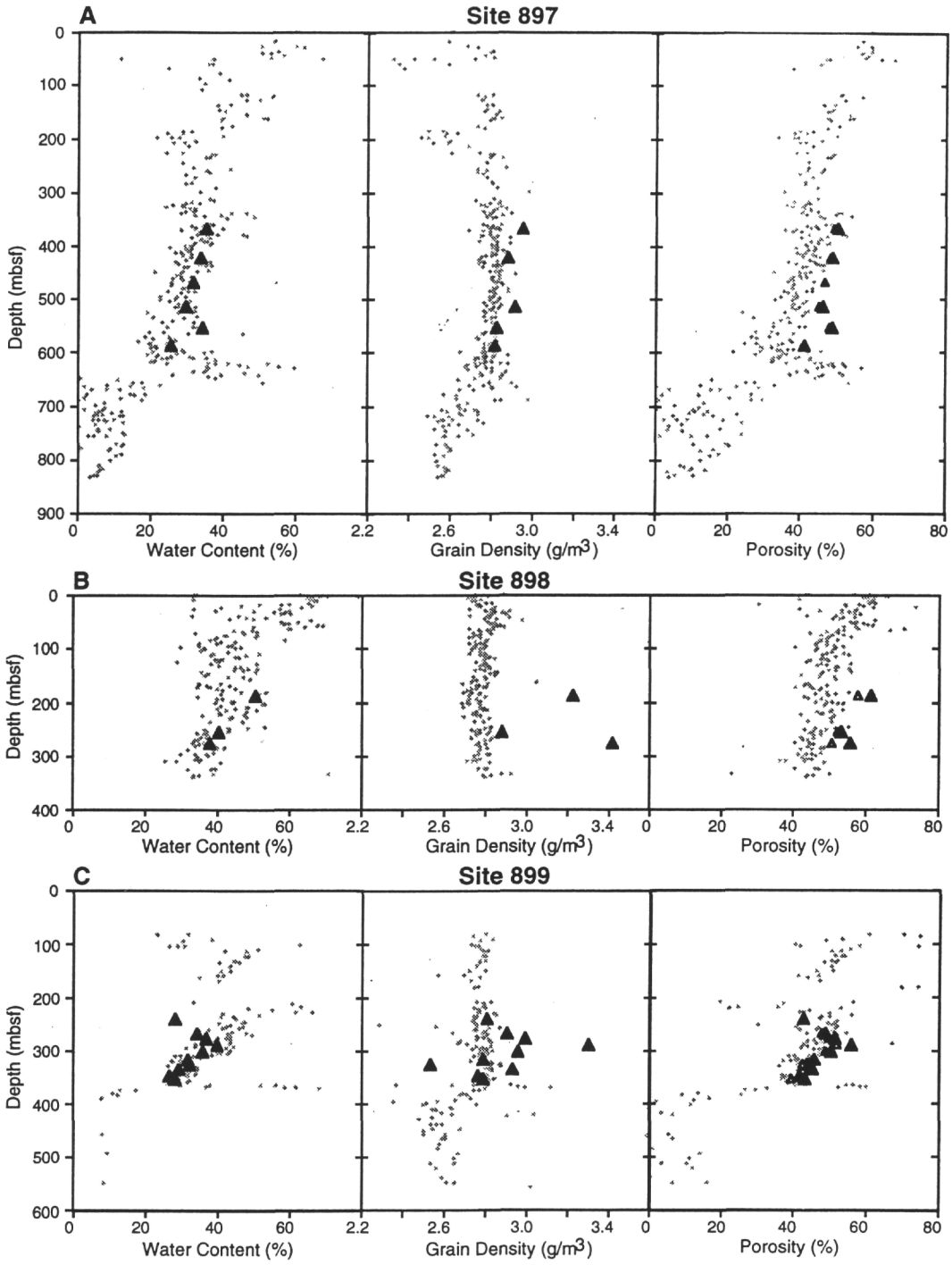

Figure 5. Laboratory-measured physical properties (solid triangles) plotted with shipboard data (shaded dots) vs. depth for each hole. **A.** Site 897. **B.** Site 898. **C.** Site 899.

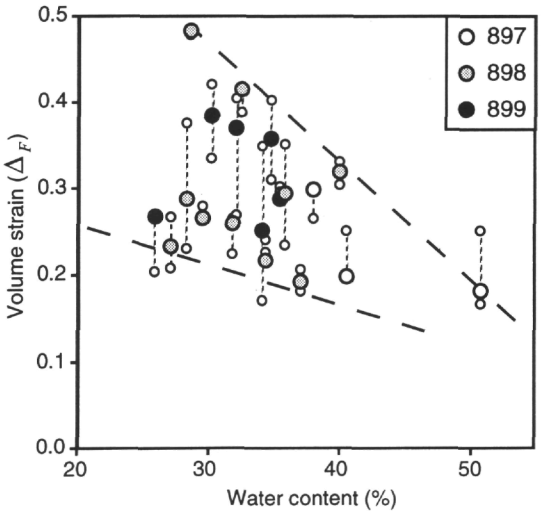

Figure 6. Apparent volume strain (Δ_F) plotted vs. water content for each sample. See Figure 2 caption for explanation of symbols. This plot shows a crude linear relationship between fabric and water content, as outlined by dashed lines.